Accepted Manuscript

Synthesis, photophysical evaluation, and computational study of 2-methoxy- and 2-morpholino pyridine compounds as highly emissive fluorophores in solution and the solid state

Masayori Hagimori, Yasuhisa Nishimura, Naoko Mizuyama, Yasuhiro Shigemitsu

Please cite this article as: Hagimori M, Nishimura Y, Mizuyama N, Shigemitsu Y, Synthesis, photophysical evaluation, and computational study of 2-methoxy- and 2-morpholino pyridine compounds as highly emissive fluorophores in solution and the solid state, *Dyes and Pigments* (2019), doi: https://doi.org/10.1016/j.dyepig.2019.107705.

1 **Synthesis, photophysical evaluation, and computational study of 2-methoxy-**

2 **and 2-morpholino pyridine compounds as highly emissive fluorophores in**

3 **solution and the solid state**

4

5 Masayori Hagimori,[a,]* Yasuhisa Nishimura,[b] Naoko Mizuyama,[c] and Yasuhiro Shigemitsu,[b,d,]*

6

7 [a]Graduate School of Biomedical Sciences, Nagasaki University, 1-7-1 Sakamoto, Nagasaki

8 852-8501, Japan

9 [b]Graduate School of Engineering, Nagasaki University, 1-14, Bunkyo-machi, Nagasaki

10 852-8131, Japan

11 [c]Clinical Research Center, Nagasaki University Hospital, 1-7-1 Sakamoto, Nagasaki 852-8501,

12 Japan

13 [d]Industrial Technology Center of Nagasaki, 2-1303-8, Ikeda, Omura, Nagasaki 856-0026,

14 Japan

15 Author E-mail address: hagimori@nagasaki-u.ac.jp (M Hagimori); shige@tc.nagasaki.go.jp

16 (Y Shigemitsu)

17

18 *Corresponding author.

19 Masayori Hagimori. Telephone: +81784417540. Fax: +81784417541. E-mail:

20 hagimori@nagasaki-u.ac.jp.

21 Yasuhiro Shigemitsu. Telephone: +81-957521133. Fax: +81-957521136. E-mail:

22 shige@tc.nagasaki.go.jp.

23

24

25 **Abstract**

26 Two 2-pyridone tautomeric analogs, methoxypyridine **4** and *N*-methylpyridone **5**, were

27 synthesized, and their spectroscopic properties were investigated both experimentally and

28 computationally. A detailed photophysical study reveals that **4** shows high fluorescence

29 quantum yields not only in chloroform but also in ethanol, and the strong fluorescence in

30 solution might be attributed to the enol form (pyridine) of the 2-pyridone. Furthermore, we

31 designed and synthesized novel 2-substitued pyridines to achieve more intense emissions in

32 both solution and the solid state. Substituent modification with phenylsulfonyl, morpholino,

33 and 4-diethylamino groups greatly affected the fluorescence properties, and methoxypyridine

34 **7** and morpholinopyridine compound **8** showed fluorescence in various solvents (Φ =

35 0.59–0.95) and the solid state (Φ = 0.12–0.15). A hypsochromic shift in the emission

36 maximum wavelength and strong fluorescence in the solid state (Φ = 0.39) were observed for

37 dimorpholinopyridine **9**. Morpholinopyridine **11** showed intense fluorescence in all nonpolar

38 and polar solvents. Systematic time-dependent density functional theory calculations were

39 performed for the compounds whose electronic and fluorescent maxima were computationally

40 reproduced with good agreement to those from experiment. In detail, the drastic difference in

41 the emission intensity between **4** and **5** in solution was successfully explained using CASSCF

42 calculations, which revealed conical intersections between the ground and the excited states.

43

44 **Keywords:** keto–enol tautomerism of 2-pyridone; pyridine; fluorescence; TDDFT; CASSCF;

45 conical intersection

46

47

48

49

1. Introduction

Fluorophores are one of the most useful materials in various chemical, biological, and material sciences because of their sensitivity, simplicity, color tunability, and low cost [1–3]. Each fluorophore, which could be an organic molecule, fluorescent protein, or quantum dot, for example, has a specific wavelength of absorbance and emission of light from the visible to near infrared region [1,4–6]. In organic molecules, particularly heterocyclic compounds, these fluorescence characteristics can be easily tuned by chemical modification [7,8]. Therefore, there has been significant effort to develop fluorophores based on organic molecules for applications as clinical diagnostic probes and organic light-emitting materials [9-15].

2-Pyridone is a nitrogen-containing heterocyclic compound and is used as a scaffold for antibacterial, anticancer, antiviral, and antimalarial agents [16–19]. In addition, 2-pyridone-based fluorophores exhibiting strong fluorescence have been reported [20–22]. Previously, we also reported several fluorescent 2-pyridone compounds, 6-(4-dialkylamino)phenyl-2-pyridones, that exhibit aggregation-induced emission enhancement (AIEE)-based fluorescence in the solid state [23,24]. These 2-pyridone compounds also exhibited fluorescence in solution, and the fluorescence quantum yields (Φ) in chloroform were very high (Φ = 0.90–0.92) [25]. However, the fluorescence intensity of the 2-pyridone compounds decreased in polar solvents such as ethanol (Φ = 0.11–0.22) [25]. It has been reported that the 2-pyridone ring has two tautomeric forms (keto and enol); the favored form depends on the solvent polarity. The 2-hyroxypyridine enol form is favored in nonpolar solvents, whereas the 2-pyridone keto form is favored in polar solvents [26–29]. Therefore, we assumed that the tautomerism of the 2-pyridone ring affects the fluorescence intensity in nonpolar and polar solvents.

Thus, to elucidate this hypothesis, we synthesized 2-pyridone tautomeric analogs, methoxypyridine compound **4** and *N*-methylpyridone compound **5**, and characterized their

3

75   fluorescence properties using photophysical studies, as well as quantum chemical

76   calculations. We have found that the enol form greatly contributes to the fluorescence intensity

77   in both nonpolar and polar solvents. In heterocyclic compounds, the arrangement of the

78   electron–donating or electron–withdrawing groups affects the intramolecular charge transfer

79   (ICT) and enhances the fluorescence intensity [22,30‑32]. In addition, we reported that the

80   steric hindrance of the alkyl group reduces the molecular aggregation of 2-pyridone and

81   induced AIEE-based fluorescence [23,25]. Most AIEE materials previously reported exhibited

82   strong fluorescence in the solid state, but their fluorescence in solution was very weak [33].

83   Therefore, the development of fluorophores exhibiting fluorescence in both solution and the

84   solid state has attracted attention. In this paper, we report the synthesis and characterization

85   of novel 2-substituted pyridine compounds (**7**–**9** and **11**) that exhibit strong fluorescence in

86   various solvents and the solid state.

87

88   **2. Materials and methods**

89   All chemicals were reagent grade and used without further purification unless otherwise

90   specified. The identification of new compounds and the measurement of the fluorescence

91   properties were performed with the following equipment. Melting points were measured using

92   a Laboratory Devices Mel-Temp II apparatus and a Mitamura Riken Kogyo Mel-Temp

93   apparatus. The NMR spectra of the compounds were obtained using Gemini 300NMR (300

94   MHz) and JEOL-GX-400 (400 MHz) spectrometers. Mass spectra (MS) and high-resolution

95   (HR) MS were obtained using a JEOL DX-303 mass spectrometer. Elemental microanalyses

96   were recorded using a Perkin-Elmer CHN analyzer.

97

4

98 *2.1 Synthesis of*

99 *6-(4-dimethylamino)phenyl-4-methylsulfanyl-2-methoxypyridine-3-carbonitrile (**4**) and*

100 *6-(4-dimethylamino)phenyl-1-methyl-4-methylsulfanyl-3-cyano-2H-pyridone (**5**)*

101 As described previously [25],

102 6-(4-(dimethylamino)phenyl)-4-(methylsulfanyl)-2-oxo-1,2-dihydropyridine-3-carbonitrile

103 (**3**; 86 mg, 0.29 mmol, 29%) was prepared by the reaction of 4'-dimethylaminoacetophenone

104 (**1a**; 1.63 g, 10.0 mmol) and 3,3-bis(methylsulfanyl)malononitrile (**2a**; 2.86 g, 10.0 mmol)

105 using powdered NaOH (1.60 g, 40 mmol) as a base in dimethyl sulfoxide (DMSO, 20 mL). To

106 a suspension of **3** (285 mg, 1.0 mmol) in DMSO (5.0 mL) and 2 N sodium hydroxide (3.0 mL),

107 dimethyl sulfate (189 mg, 1.5 mmol) was added over 20 min, and the resulting suspension was

108 stirred for 1.5 h. After pouring 50 mL water into the reaction mixture, a precipitate formed,

109 which was collected by filtration and washed several times with water. Purification by silica gel

110 column chromatography (10 g of silica gel) eluted with toluene gave **4** (86 mg, 0.29 mmol,

111 29%) and that with toluene and methanol (ratio 4:1) gave **5** (107 mg, 0.36 mmol, 36%). An

112 analytical sample was recrystallized from methanol to give pale yellow needles of **4** (mp

113 171–172 °C). IR (KBr, cm^{-1}): 2921, 2211, 1609, 1566, 1539, 1364, 1187, 1166, 1034, 812.

114 ^{1}H-NMR (CDCl$_3$, 400 MHz): 2.62 (3H, s, SMe), 3.06 (6H, s, NMe$_2$), 4.11 (3H, s, OMe), 6.75

115 (2H, d, J = 9.1 Hz, 3', 5'-H), 7.06 (1H, s, 5-H), 7.96 (2H, d, J = 9.1 Hz, 2', 6'-H). ^{13}C-NMR

116 (CDCl$_3$, 100 MHz): 14.4, 41.3, 54.2, 106.4, 114.5, 128.7, 157.1, 164.4. MS m/z: 300 (M$^+$ + 1,

117 70), 299 (M$^+$, 100), 298 (83), 282 (11), 240 (22), 236 (11). Anal. Calcd for C$_{16}$H$_{17}$N$_3$SO =

118 299.1092: C, 64.19%; H, 5.72%; N, 14.04%. Found: C, 64.36%; H, 5.74%; N, 14.10%. An

119 analytical sample was recrystallized from methanol to give yellow needles of **5** (mp

120 218–220 °C). IR (KBr, cm^{-1}): 3250, 3000, 2910, 2820, 2210 (CN), 1640 (C=O), 1600, 1510,

121 1490, 1440, 1420, 1360, 1310, 1290, 1240, 1215, 1180, 1060, 1040. ^{1}H-NMR (CDCl$_3$, 400

122 MHz): 2.52 (3H, s, Me), 3.07 (6H, s, NMe$_2$), 3.44 (3H, s, NMe), 6.05 (1H, s, 5-H), 6.80 (2H, d,

5

123 J = 9.1 Hz, 3',5'-H), 7.27 (2H, d, J = 9.1 Hz, 2', 6'-H). ^{13}C-NMR (CDCl$_3$, 100 MHz): 14.4,

124 34.9, 40.3, 95.68, 103.5, 111.9, 115.0, 129.3, 151.2, 154.3, 160.7, 161.1. MS m/z: 300 (M$^+$ + 1,

125 47), 299 (M$^+$, 100), 298 (13), 127 (11), 112 (12), 99 (15). Anal. Calcd for C$_{16}$H$_{17}$N$_3$SO =

126 299.1092: C, 64.19%; H, 5.72%; N, 14.04%. Found: C, 64.01%; H, 5.68%; N,13.86%.

127

128 *2.2 Synthesis of*

129 *6-(4-dimethylamino)phenyl-4-methylsulfanyl-3-phenylsulfonyl-2-methoxypyridine (7)*

130 As described previously [25],

131 6-(4-(dimethylamino)phenyl)-4-(methylsulfanyl)-3-(phenylsulfonyl)pyridin-2(1H)-one (**6**)

132 (0.96 g, 2.40 mol) was prepared by the reaction of **1a** (1.63 g, 10.0 mmol) and

133 3,3-bis(methylsulfanyl)-2-phenylsulfonyl-acrylonitrile (**2b**; 1.43 g, 5.0 mmol) using powdered

134 NaOH (1.12 g, 28 mmol) and morpholine (1.5 g, 17.2 mmol) in DMSO (20 mL). To a

135 suspension of **6** (150 mg, 3.75 mmol) in DMSO (10 mL) and a solution of 1 N sodium

136 hydroxide (6.0 mL), dimethyl sulfate (250 mg, 1.5 mmol) was added over 30 min, and the

137 resulting suspension was stirred for 1.5 h. After the addition of 50 mL water to the reaction

138 mixture, the formed precipitate was collected by filtration and washed several times with water.

139 Purification by silica gel column chromatography (10 g of silica gel) eluted with toluene gave

140 pale yellow needles of **7** (65 mg, 0.157 mmol, 42%, mp 194–195 °C). IR (KBr, cm^{-1}): 2920,

141 2367, 2337, 1615, 1527, 669. ^{1}H-NMR (CDCl$_3$, 400 MHz): 2.55 (3H, s, Me), 3.07 (6H, s,

142 NMe$_2$), 3.93 (3H, s, OMe), 6.73 (2H, d, J = 9.3 Hz, 3",5"-H), 7.11 (1H, s, 5-H), 7.48 (2H, m,

143 3',5'-H), 7.56 (1H, m, 4'-H), 7.91 (2H, d, J = 9.3 Hz, 2",6"-H), 8.06 (2H, m, 2',6'-H).

144 ^{13}C-NMR (CDCl$_3$, 100 MHz): 16.0, 16.1, 40.1, 40.1, 53.8, 107.0, 107.1, 111.7, 124.5, 127.6,

145 128.2, 128.4, 142.7, 151.8, 155.8, 157.4, 160.9. MS (FAB) m/z: 415 (M + H$^+$).

146

147 *2.3 Synthesis of 6-(4-(dimethylamino)phenyl)-4-(methylsulfanyl)-2-morpholinonicotinonitrile*

148 *(8) and 6-(dimethylamino)phenyl-2,4- dimorpholinopyridine-3-carbonitrile (9)*

149 A solution of **1a** (1.63 g, 10.0 mmol), **2a** (2.86 g, 10.0 mmol), and NaOH (1.60 g, 40 mmol) in

150 DMSO (20 mL) was stirred at 10–15 °C for 5 h. After the addition of 300 mL of ice water to the

151 reaction mixture, the mixture was acidified with 10% hydrochloric acid. The resulting

152 caramel-colored intermediate was collected by decantation and washed with ice cold water

153 several times. A solution of the intermediate in water and morpholine (3.0 g, 34.4 mmol) was

154 heated for 20 min at about 200 °C. After filtration, the filtrate was concentrated in vacuo.

155 Purification by silica gel column chromatography (20 g of silica gel) eluted with

156 toluene:methanol (4:1) gave **3** (960 mg, 2.40 mmol, 24%), **8** (92 mg, 0.26 mmol, 2.6%), and **9**

157 (82 mg, 0.21 mmol, 2.1%). An analytical sample was recrystallized from methanol to give

158 colorless needles of **8** (mp 167–168 °C). IR (KBr, cm^{-1}): 2854, 2367, 2336, 1570, 1532, 1112.

159 ^{1}H-NMR (CDCl$_3$, 400 MHz): 3.04 (6H, s, NMe$_2$), 3.42 (2H, m, N–CH$_2$–), 3.70 (2H, m,

160 N–CH$_2$–), 3.87 (4H, m, –CH$_2$–O–CH$_2$–), 6.73 (2H, d, J = 8.8 Hz, 3', 5'-H), 7.91 (2H, d, J = 8.8

161 Hz, 2', 6'-H). ^{13}C-NMR (CDCl$_3$, 100 MHz): 14.5, 40.4, 48.8, 66.8, 89.3, 104.9, 112.2, 116.8,

162 128.5, 157.3, 157.4, 161.6. MS m/z: 355 (M$^+$ + 1, 28), 354 (M$^+$, 100), 339 (14), 324 (16), 323

163 (20), 297 (60), 296 (87), 269 (14), 222 (11). Anal. Calcd for C$_{19}$H$_{22}$N$_4$SO = 354.1514: C,

164 64.38%; H, 6.26%; N, 15.81%. Found: C, 64.32%; H, 6.22%; N, 15.85%. In addition, an

165 analytical sample was recrystallized from methanol to give colorless needles of **9** (mp

166 197–198 °C). IR (KBr, cm^{-1}): 2966, 2851, 2193 (CN), 1608, 1570, 1536, 1112, 819. ^{1}H-NMR

167 (CDCl$_3$, 400 MHz): 3.04 (6H, s, NMe$_2$), 3.44 (4H, m, 2 × N–CH$_2$–), 3.70 (4H, m, 2 × N–CH$_2$–),

168 3.88 (8H, m, 2 × O–CH$_2$–). ^{13}C-NMR (CDCl$_3$, 100 MHz): 40.4, 49.2, 50.6, 66.6, 66.8, 82,3,

169 98.2, 112.0, 118.8, 128.3, 158.9, 163.7, 163.9. MS m/z: 394 (M$^+$ + 1, 24), 393 (M$^+$, 94), 336

170 (41), 335 (100), 315 (16), 299 (29). Anal. Calcd for C$_{22}$H$_{27}$N$_5$O$_2$ = 393.2165: C, 67.15%; H,

171 6.92%; N, 17.80%. Found: C, 67.01%; H, 7.05%; N, 17.77%.

172

173 *2.4 Synthesis of*

174 *6-(4-diethylamino)phenyl-4-methylsulfanyl-2-morpholinopyridine-3-carbonitrile (**11**)*

175 Compound **11** (54 mg 0.141 mmol, 2.8% yield) was prepared from

176 4-(diethylamino)phenylacetophenone (**1b**, 0.86 g, 5.0 mmol) and **2a** (0.85 g, 5.0 mmol) in a

177 manner similar to that described for the synthesis of **8**. An analytical sample was recrystallized

178 from dimethylformamide (DMF) and methanol to give pale yellow needles (mp 137–138 °C).

179 IR (KBr, cm^{-1}): 2898, 2845, 2200 (CN), 1608, 1537, 1524, 1419, 1366, 814. ^{1}H-NMR (CDCl$_3$,

180 400 MHz): 1.21 (6H, t, J = 7.0 Hz, $2 \times$ CH$_2$-$\underline{\text{CH}_3}$), 2.60 (3H, s, SMe), 3.43 (4H, d, J = 7.0 Hz,

181 $2 \times$ N-CH$_2$-), 3.73 (4H, t, J = 5.1 Hz, $2 \times$ -CH$_2$-N), 3.68 (4H, t, J = 5.1 Hz, $2 \times$ O-CH$_2$-), 6.71

182 (2H, d, J = 9.2 Hz, 3', 5'-H), 6.93 (1H, s, 5-H), 7.91 (2H, d, J = 9.1 Hz, 2', 6'-H). ^{13}C-NMR

183 (DMSO-d6, 100MHz): 12.4, 13.6, 43.7, 48.5, 65.94, 87.5, 104.6, 110.9, 116.6, 123.1, 129.0,

184 149.1, 156.7, 157.2, 161.1. Anal. Calcd for C$_{21}$H$_{22}$N$_2$S$_2$O$_3$ = 382.1827: C, 65.94%; H, 6.85%;

185 N, 14.65%. Found: C, 65.78%; H, 6.76%; N, 14.63%.

186

187 *2.5. Fluorescence measurements*

188 The solid-state fluorescence of powdered samples was measured in a Shimadzu RF-5300pc

189 fluorescence spectrometer. After the excitation spectrum had been measured by scanning at the

190 fluorescent wavelength, the fluorescence spectrum was obtained using the excitation

191 wavelength. The fluorescence spectra in solution were obtained in a manner similar to that in

192 the solid state. To measure the fluorescence in solution, the concentrations of samples were

193 adjusted using a molar absorption coefficient of 0.05. The fluorescence spectra in solution were

194 obtained in the same way as the solid-state measurements. Fluorescence quantum yields were

195 determined using an Absolute PL Quantum Yield Measurement System (C9920-01) from

196 Hamamatsu Photonics.

197

198   *2.6. X-ray crystallography*

199   X-ray diffractometry (XRD) data were obtained with a Rigaku Saturn724 diffractometer using

200   multilayer mirror monochromated Mo-Kα radiation at -179 $\pm$ 1 °C, and all calculations were

201   conducted using CrystalClear (Rigaku). The structure of **8** (CCDC-1896939) can be obtained

202   from the Cambridge Crystallographic Data Centre via request

203   (www.ccdc.cam.au.uk/data_request/cif).

204   Crystal data for **8**: A crystal was obtained by recrystallization from MeOH/acetonitrile (1:1),

205   which yielded colorless blocks of formula $C_{19}H_{22}N_4OS$ having approximate dimensions of

206     $0.270 \times 0.080 \times 0.020$ mm. The crystal was mounted on a glass fiber for data collection.

207   Crystal data formula weight: 354.47; crystal color: colorless; habit: block; crystal system:

208   triclinic; lattice type: primitive; lattice parameters: $a = 11.072(3)$ Å, $b = 11.374(3)$ Å, $c =$

209     $15.493(4)$ Å, $\beta = 90.259(3)°$, V $= 1819.7(7)$ Å^3; space group: *P*-1 (#2); Z-value: 4; calculated

210   density (D_{calcd}): 1.294 g cm^{-3}; $F(000) = 752.00$; and absorption coefficient (μ(Mo-Kα)) = 1.923

211   cm^{-1}.

212

213   **3. Computational details**

214   The ground state geometries of all molecules in vacuo were fully optimized at the density

215   functional theory (DFT) B3LYP/6-311++G(d,p) level of theory. The lowest excited states (S_1)

216   were geometrically optimized in vacuo by means of time-dependent DFT (TDDFT)

217   calculations at the B3LYP/6-31+G(d,p) level of theory using the default convergence criterion

218   for force and displacement implemented in Gaussian 09 [34]. For the optimized geometries, the

219   S_0–S_1 (absorption) and the S_1–S_0 transition energies (fluorescence) were evaluated at the

220   TDDFT/6-311++G(d,p) and 6-31+(d,p) levels using the B3LYP [35], CAM-B3LYP [36],

221   PBEPBE [37], M06 [38], and M06-2X [38] exchange–correlation (XC) functionals. Solvent

222   effects were taken into account using the polarizable continuum model (PCM).

223   In the detailed study of **4** and **5**, the relaxation paths in S_1 were explored from the

224   Franck–Condon (FC) state to the S_1-minimum and to the minimum energy conical

225   intersections (MECIs) [39], respectively. The MECIs were located using MOLPRO [40] at the

226   CASSCF(8,7)/def2-SV(P) level of theory. The single point calculations were carried out at the

227   TDDFT(B3LYP)/def-TZVP level of theory using the TURBOMOLE suite of program [41] to

228   refine the energies of the S_1-FC, the S_1-minima, and the S_0/S_1-MECIs states.

229

230   **4. Results and discussion**

231   *4.1 Synthesis and fluorescence of 2-pyridone tautomeric analogs (**4** and **5**)*

232   The synthesis of 2-methoxypyridine compound **4** and *N*-methylpyridone compound **5** is

233   shown in Scheme 1. The reaction of 4'-dimethylaminoacetophenone (**1a**) with cyano-keten

234   *S,S*-acetal (**2a**) in the presence of sodium hydroxide as a base in DMSO at room temperature

235   followed by the addition of 10% hydrochloric acid yielded 2-pyridone compound **3** in 29%.

236   The methylation of **3** was achieved using dimethyl sulfate in the presence of sodium

237   hydroxide, and the resultant mixture of **4** and **5** was easily separated by silica gel column

238   chromatography. Methoxypyridine compound **4** was firstly eluted using toluene in 29% yield,

239   and *N*-methylpyridone compound **5** was subsequently eluted using a mixture of toluene and

240   methanol (ratio 4:1) in 36% yield. Next, we analyzed the fluorescence properties of these

241   compounds in two solutions (chloroform and ethanol) and the solid state. The absorption

242   maxima (λ_{max}), emission maxima (Em_{max}), and Φ values of compounds **3**–**5** are listed in Table

243   1. The Em_{max} values of **4** and **5** were observed at 461 nm in chloroform and at 491 nm in

244   ethanol, which is a hypsochromic shift of the same extent as that induced by the *N*- or *O*-

245   methylation of **3**. The pyridine form compound **4** exhibited strong fluorescence in both

246   chloroform ($\Phi > 0.99$) and ethanol ($\Phi = 0.61$), whereas the Φ values of the pyridone form

247 compound **5** were very low in both chloroform ($\Phi = 0.12$) and ethanol ($\Phi = 0.05$). Because

248 the fluorescence of 2-pyridone **3** was intense in chloroform ($\Phi = 0.90$) but weak in ethanol

249 ($\Phi = 0.11$), we speculated that the fluorescence of 2-pyridones **3** in chloroform is due to the

250 pyridine form (the enol of 2-pyridone), whereas that in ethanol is due to the pyridone form

251 (the keto of 2-pyridone). In the solid state, the Em_{max} values of **4** and **5** also occurred at

252 shorter wavelengths than that of **3**; however, *N*-methylpyridone compound **5** exhibited

253 stronger fluorescence ($\Phi = 0.18$) than methoxypyridine compound **4** ($\Phi = 0.03$). In a

254 previous study, we revealed that 2-pyridones, including compound **3** ($\Phi = 0.17$), show

255 moderate fluorescence in the solid state, and we also reported that the keto–enol equilibrium

256 of these 2-pyridones is remarkably shifted to the 2-pyridone tautomer on the basis of X-ray

257 crystal structure analysis [25]. Therefore, the fluorescence intensity of **5** in the solid state is

258 consistent with our previous results.

259

260

261   **Scheme 1.**

262   **Table 1.**

263

264 *4.2 Synthesis and fluorescence of 2-substituted pyridines*

265 The molecular packing arrangement and orientation caused by substituents often influence

266 the fluorescence intensity in the solid state [25,33]. We previously reported that the

267 introduction of sulfonyl group disrupts the molecular planarity of 2-pyridones, thus

268 decreasing the π—π stacking interactions [25,42]. Therefore, compounds showing strong

269 fluorescence in both solution and the solid state could be developed by introducing a

270 substituent into the pyridine that exhibits strong fluorescence in solution. Thus, we prepared a

271 series of 2-substitued pyridine compounds: **7**–**9** and **11** (Scheme 2). After sulfonyl pyridone

272   compound **6** had been prepared from the reaction of **1a** with **2b**, the methylation of **6** using

273   dimethyl sulfate was conducted, similar to the syntheses of **4** and **5**. In this reaction, however,

274   methoxypyridine compound **7** was only obtained in 42% yield. Morpholinopyridine

275   compounds **8** and **9** were prepared from **1a** and **2a** using morphine. After filtration the major

276   products, 3,2-morpholinopyridine compound **8** and 2,4-dimorpholinopyridine compound **9**,

277   were obtained from the filtrate in 2.6% and 2.1% yields, respectively. Fig. 1 shows the X-ray

278   crystal structure of compound **8**. We previously reported that the replacement of the

279   dimethylamino group with a diethylamino group at the 6-positon of the 2-pyridone ring

280   reduces the molecular aggregation, and diethylamino 2-pyridone compound **10** showed

281   stronger fluorescence than dimethylamino 2-pyridone compound **3** in solution [25,43].

282   6-(4-Diethylamino)phenyl-2-morpholinopyridine compound **11** was obtained in a similar

283   manner from the reaction of **1b** and **2a**.

284

285

286   **Scheme 2.**

287   **Fig. 1.**

288

289   The fluorescence properties of **7**–**9** and **11** in solution (chloroform and ethanol) and the solid

290   state are summarized in Table 2. The Φ values of phenylsulfonyl-methoxypyridine compound

291   **7** were 0.95 in chloroform and 0.62 in ethanol, which are comparable to that of

292   methoxypyridine compound **4**. Meanwhile, the solid state fluorescence of **7** was increased to

293   0.15, suggesting that molecular planarity disruption is induced by the introduction of the

294   phenylsulfonyl group, as in the 2-pyridones [25]. Compounds **8** and **9** contain a morpholino

295   group instead of a methoxy group and also exhibited strong blue fluorescence in the solid

296   state (Fig 2), especially dimorpholinopyridine compound **9**, which showed intense

297 fluorescence ($\Phi = 0.39$). In contrast, the Φ values in solution decreased with increasing

298 number of morpholino groups. The Em_{max} of **9** exhibits hypsochromic shifts about 50–65 nm

299 in solution. 4-Diethylamino morpholinopyridine compound **11** exhibited stronger

300 fluorescence than 4-dimethylamino morpholinopyridine compound **8** in solution and the solid

301 state. The emission maximum wavelengths of **11** in chloroform and ethanol were

302 hypsochromically shifted by about 25 nm, and, interestingly, the solid state emission

303 wavelength was bathochromically shifted by about 55 nm. The results indicated that the

304 arrangement of substituents might enable the development of fluorophores exhibiting strong

305 fluorescence in both solution and the solid state, and these compounds had a potential to be a

306 fluorophore for clinical diagnostic probes and organic light-emitting materials.

307

308 **Table 2.**

309 **Fig.2**

310

311 *4.3 Solvatochromic effects on absorption and emission*

312 The fluorescence solvatochromic effects depend on the chemical structure and arrangement

313 of the substituents. We investigated the solvatochromism of compounds **4**, **5**, **7**–**9**, and **11** in

314 various solvents except for water. All compounds were hardly soluble in water. The

315 absorption maxima, emission maxima and fluorescence spectra in nonpolar, aprotic polar, and

316 protic polar solvents are given in Table 3 and Fig. 3. The absorption maximum wavelengths

317 of all compounds did not change significantly, but the emission maximum wavelengths of

318 these compounds were bathochromically shifted as the polarity of the solvent increased. As a

319 consequence, their Stokes shifts increased in polar solvents. The fluorescence intensity of

320 pyridine compounds **4**, **7**–**9**, and **11** were stronger than that of the 2-pyridone compound **5** in

321 all solvents (Table 2). The Φ values of **4**, **7**, and **8** in nonpolar and aprotic polar solvents were

13

322 higher than those in a protic solvent (ethanol). On the other hand, dimorpholinopyridine

323 compound **9** exhibited strong fluorescence in chloroform and DMSO. 4-Diethylamino

324 morpholinopyridine compound **11** exhibited intense fluorescence in all solvents, indicating

325 that it is possible to develop an efficient and stable emissive fluorophore unaffected by

326 solvent properties.

327

328

329 **Table 3**

330 **Fig.3**

331

332 *4.4 Computational analysis of the spectroscopic properties: A drastic difference in emission*

333 *intensity between **4** and **5***

334 Regarding the absorption spectra, Table 4 lists the computed first intense λ_{max} values of all

335 compounds. Among the tested XC functionals, the best agreement between the experimental

336 and computed λ_{max} values were obtained using B3LYP. The computed maxima exhibited red

337 shifting in order of CAM-B3LYP < M06-2X < M06 < B3LYP < PBEPBE. The long-range

338 corrected functional CAM-B3LYP severely overestimated the vertical transition energies,

339 whereas PBEPBE underestimated the energies used to predict the λ_{max}. The inclusion of

340 solvent effects via the PCM resulted in a red shift in the B3LYP-maxima from 16 nm (**9**) to 41

341 nm (**5**) in chloroform. The B3LYP λ_{max} dependency on the two basis set (6-31+(d,p),

342 6-311++G(d,p)) is limited to a variation of 2 nm for all the compounds, as shown in Table 5.

343 Both **4** and **5** undergo considerable intramolecular electron transfer from the dialkylaminoaryl

344 moiety to methylthioaryl moiety upon S_0->S_1 excitation, as shown in Fig. 4. The two molecules,

345 however, have contrasting molecular structures derived from the steric hindrance around the

346 central single bond. For example, **4** retains a nearly flat structure, whereas **5** has a considerable

347 twist around the bond owing to the repulsion between the methylthio group and the counterpart

348 aryl group, as shown in Fig. 5.

349

350 **Table 4**

351 **Table 5**

352 **Fig. 4**

353 **Fig. 5**

354

355 For the fluorescence spectra, Table 6 shows the computed first intense emission maxima for all

356 compounds. The 6-31+G(d,p) basis set was uniformly employed considering the minor basis

357 set dependency mentioned above. The prediction trend is similar to that observed for

358 absorption, and λ_{max} shifted bathochromically in order of CAM-B3LYP < M06-2X < M06 <

359 B3LYP < PBEPBE. The best agreement exists between B3LYP (overestimation) and PBEPBE

360 (underestimation), excluding **4** and **5**, whose maxima were consistently predicted at shorter

361 wavelength using all XC functionals.

362

363 **Table 6**

364

365 Notably, **4** and **5** exhibited contrasting emission intensities in solution despite only differing in

366 the modification at the nitrogen atom of the pyridine ring. We attempted to elucidate the

367 mechanism by locating the S_1-minima and the S_0/S_1 crossing seam along with the relaxation

368 pathways. The non-radiative decay channels occur along the seam of the S_0/S_1 conical

369 intersections (CIs), which are represented by its minimum energy points (MECIs). The

370 S_0/S_1-MECI geometries of **4** and **5** optimized at the CASSCF(8,7)/def2-SV(P) level of theory,

371 are shown in Fig. 6.

15

372

373 **Fig. 6**

374

375 Our calculations clearly show the drastic differences in the energy gap between the S_1-FC and

376 the S_0/S_1-MECI for the two molecules with severely distorted pyridine rings, as shown in Fig. 7.

377 Compound **4** has a large gap, which is sufficient to separate the two states and prohibit the

378 interconversion between S_1-FC and the S_0/S_1-MECI states, resulting in **4** being highly emissive.

379 Conversely, **5** has a small gap, which allows the two states to be mutually accessible, and the S_1

380 excited molecule can radiationlessly return to the ground state via the S_0/S_1-MECI. The S_0

381 energy is not exactly identical to the S_1 energy because the optimized MECI geometry was

382 obtained at the CASSCF(8,7)/def2-SV(P) level of theory (not B3LYP/def-TZVP).

383

384 **Fig. 7**

385

386 In the solid state, the fluorescence intensity of **4** became weak, whereas that of **5** was enhanced

387 in comparison with that in ethanol. This indicates that the intermolecular stacking interactions

388 dominate the emission intensities of the two molecules. That is, **4**, which has a planar structure,

389 can stack in the solid state, which activates non-radiative energy dissipation pathways, whereas

390 the emission enhancement of **5**, which has a twisted structure, is caused by the inaccessibility

391 of the S_0/S_1-MECI state owing to intermolecular steric hindrance. This is consistent with the

392 observation of the emission enhancement of **9**, which has two bulky moieties, compared to the

393 emissions of **4** and **5**.

394

395 **5. Conclusion**

396 To elucidate the influence of the keto–enol tautomerism of 2-pyridone rings on the

16

397 fluorescence intensity, we synthesized two 2-pyridone tautomeric analogs, methoxypyridine

398 compound **4** and *N*-methylpyridone compound **5**, and demonstrated that compound **4** (enol

399 form) shows strong fluorescence in both nonpolar and polar solvents, whereas **5** shows quite

400 weak fluorescence. The computational analysis successfully explained the drastic difference in

401 the fluorescence intensities between the two molecules in solution, which arises because of the

402 energy gap between the S_1-FC and the S_0/S_1-MECI states of the two molecules. That is, **4** has a

403 gap that is sufficiently large to separate the two states and prohibit their interconversion, thus

404 maintaining **4** in a highly emissive state. On the other hand, **5** has a small gap that allows the

405 two states to transition between each other, and the molecule returns to the ground state via the

406 S_0/S_1-MECI radiationlessly. On the basis of these results, novel 2-substituted pyridine

407 compounds **7**–**9** and **11** were synthesized from dialkylaminoacetophenones with cyanoketen

408 *S,S*-acetals, and their fluorescence properties in solution and the solid state were evaluated.

409 The substituents including phenylsulfonyl, morpholino, and 4-diethylamino groups greatly

410 affected the fluorescence intensity in solution and the solid state. 2-Methoxypyridine

411 compound **7** and 2-morpholinopyridine compound **8** exhibited solid-state fluorescence and a

412 high fluorescence quantum yield in solution. Although its solution fluorescence was

413 decreased, dimorpholinopyridine compound **9** exhibited strong fluorescence ($\Phi = 0.39$) in the

414 solid state. In addition, a 4-diethylamino morpholinopyridine compound having

415 4-diethylamino group (**11**) exhibited intense fluorescence in all solvents because aggregation

416 was prevented. These findings may be useful for the development of fluorophores exhibiting

417 strong fluorescence in solution and the solid state.

418

421

17

422 **References**

423 [1] Chen X, Wang F, Hyun JY, Wei T, Qiang J, Ren X, Shin I, Yoon J. Recent progress

424   in the development of fluorescent, luminescent and colorimetric probes for detection

425   of reactive oxygen and nitrogen species. Chem Soc Rev 2016;45(10):2976–3016.

426 [2] Specht EA, Braselmann E, Palmer AE. A critical and comparative review of

427   fluorescent tools for live-cell imaging. Annu Rev Physiol 2017;79:93–117.

428 [3] Basabe-Desmonts L, Reinhoudt DN, Crego-Calama M. Design of fluorescent

429   materials for chemical sensing. Chem Soc Rev 2007;36(6):993–1017.

430 [4] Shcherbakova DM, Baloban M, Emelyanov AV, Brenowitz M, Guo P, Verkhusha VV.

431   Bright monomeric near-infrared fluorescent proteins as tags and biosensors for

432   multiscale imaging. Nat Commun 2016;7:12405.

433 [5] Zhao P, Xu Q, Tao J, Jin Z, Pan Y, Yu C, Yu Z. Near infrared quantum dots in

434   biomedical applications: current status and future perspective. Wiley Interdiscip Rev

435   Nanomed Nanobiotechnol 2018;10(3):e1483.

436 [6] Wang X, Liu L, Zhu S, Li L. Fluorescent platforms based on organic molecules for

437   chemical and biological detection. Phys Status Solidi RRL 2018:1800521.

438 [7] He L, Lin W, Xu Q, Ren M, Wei H, Wang JY. A simple and effective "capping"

439   approach to readily tune the fluorescence of near-infrared cyanines. Chem Sci

440   2015;6(8):4530–36.

441 [8] Sueki S, Takei R, Zaitsu Y, Abe J, Fukuda A, Seto K, Furukawa Y, Shimizu I.

442   Synthesis of 1,4-dihydropyridines and their fluorescence properties. Eur J Org Chem

443   2014;2014(24):5281–301.

444 [9] Duan L, Qiao J, Sun Y, Qiu Y. Strategies to design bipolar small molecules for

445   OLEDs: donor-acceptor structure and non-donor-acceptor structure. Adv Mater

446   2011;23(9):1137–44.

447 [10] Terai T, Nagano T. Small-molecule fluorophores and fluorescent probes for

448   bioimaging. Pflugers Arch 2013;465(3):347–59.

449 [11] Zhu H, Fan J, Du J, Peng X. Fluorescent probes for sensing and imaging within

450   specific cellular organelles. Acc Chem Res 2016;49:2115–26.

451 [12] Hagimori M, Taniura M, Mizuyama N, Karimine Y, Kawakami S, Saji H, Mukai T.

452   Synthesis of a novel pyrazine–pyridone biheteroaryl-based fluorescence sensor and

453   detection of endogenous labile zinc ions in lung cancer cells. Sensors 2019;19(9):

454   2049–60.

455 [13] Duan C, Won M, Verwilst P, Xu J, Kim HS, Zeng L, Kim JS. In vivo imaging of

456   endogenously produced HClO in zebrafish and mice using a bright, photostable

457   ratiometric fluorescent probe. Anal Chem 2019;91:4172–8.

458 [14] Duan C, Zhou Y, Shan GG, Chen Y, Zhao W, Yuan D, Zeng L, Huang X, Niu G.

459   Bright solid-state red-emissive BODIPYs: facile synthesis and their high-contrast

460   mechanochromic properties. J Mater Chem C 2019;7:3471—8.

461 [15] Duan C, Zhang JF, Hu Y, Zeng L, Su D, Bao GM. A distinctive near-infrared

462   fluorescence turn-on probe for rapid, sensitive and chromogenic detection of sulfite

463   in food. Dyes Pigm 2019;162:459-65.

464 [16] Li Q, Mitscher LA, Shen LL. The 2-pyridone antibacterial agents: bacterial

465   topoisomerase inhibitors. Med Res Rev 2000;20(4):231–93.

466 [17] Li LN, Wang L, Cheng YN, Cao ZQ, Zhang XK, Guo XL. Discovery and

467   characterization of 4-hydroxy-2-pyridone derivative sambutoxin as a potent and

468   promising anticancer drug candidate: Activity and molecular mechanism. Mol Pharm

469   2018;15(11):4898–911.

470 [18] Jia H, Song Y, Yu J, Zhan P, Rai D, Liang X, Ma C, Liu X. Design, synthesis and

471   primary biological evaluation of the novel 2-pyridone derivatives as potent

472   non-nucleoside HBV inhibitors. Eur J Med Chem 2017;136:144–53.

473 [19] Isaka M, Tanticharoen M, Kongsaeree P, Thebtaranonth Y. Structures of

474   cordypyridones A-D, antimalarial N-hydroxy- and N-methoxy-2-pyridones from the

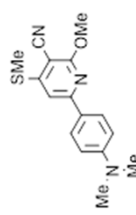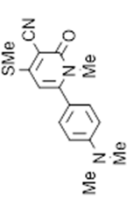475   insect pathogenic fungus Cordyceps nipponica. J Org Chem 2001;66:4803–8.
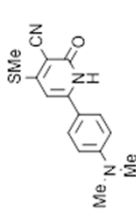
476 [20] Ershov OV, Fedoseev SV, Ievlev MYu, Belikov MYu. 2-Pyridone-based
477   fluorophores: Synthesis and fluorescent properties of pyrrolo[3,4-c]pyridine
478   derivatives. Dyes Pigm 2016;134:459–64.

479 [21] Sellstedt M, Nyberg A, Rosenbaum E, Engström P, Wickström M, Gullbo J,
480   Bergström S, Johansson L. B.-Å, Almqvist F. Synthesis and characterization of a
481   multi ring-fused 2-pyridone-based fluorescent scaffold. Eur J Org Chem
482   2010;2010(32):6171–8.

483 [22] Hagimori M, Uto T, Mizuyama N, Temma T, Yamaguchi Y, Tominaga Y, Saji H.
484   Fluorescence ON/OFF switching Zn^{2+} sensor based on pyridine–pyridone scaffold.
485   Sens Act B Chem 2013;181:823–8.

486 [23] Shigemitsu Y, Hagimori M, Mizuyama N, Wang BC, Tominaga Y. Theoretical
487   interpretations of electronic and fluorescence spectra of new 2(1H)-pyridone
488   derivatives in solution and solid state. Dyes Pigm 2013;99(3):940–9.

489 [24] Hagimori M, Temma T, Mizuyama N, Uto T, Yamaguchi Y, Tominaga Y, Mukai T,
490   Saji H. A high-affinity fluorescent Zn^{2+} sensor improved by the suppression of
491   pyridine-pyridone tautomerism and its application in living cells. Sens Act B Chem
492   2015;213:45-52.

493 [25] Hagimori M, Shigemitsu Y, Murakami R, Yokota K, Nishimura Y, Mizuyama N,
494   Wang BC, Tai CK, Wang SL, Shih TL, Wu KD, Huang ZS, Tseng SC, Lu JW, Wei
495   HH, Nagaoka J, Mukai T, Kawashima S, Kawashima K, Tominaga Y.
496   2-Pyridone-based fluorophores containing 4-dialkylamino-phenyl group: Synthesis
497   and fluorescence properties in solutions and in solid state. Dyes Pigm
498   2016;124:196–202.

499 [26] Wong MW, Wiberg KB, Frisch MJ. Solvent effects. 3. Tautomeric equilibria of
500   formamide and 2-pyridone in the gas phase and solution: an ab initio SCRF study. J
501   Am Chem Soc 1992;114:1645–52.

502 [27] Forlani L, Cristoni G, Boga C, Todesco PE, Del Vecchio E, Selva S, Monari M.

503   Reinvestigation of tautomerism of some substituted 2-hydroxypyridines. Arkivoc
504   2002;XI:198–215.

505   [28]   Hejazi SA, Osman OI, Alyoubi AO, Aziz SG, Hilal RH. The thermodynamic and
506   kinetic properties of 2-hydroxypyridine/2-pyridone tautomerization: A theoretical and
507   computational revisit. Int J Mol Sci 2016;17(11):E1893.

508   [29]   Frank J, Katritzky AR. Tautomeric pyridines. Part XV. Pyridone–hydroxypyridine
509   equilibria in solvents of differing polarity. J Chem Soc Perkin Trans 2 1976:1428–31.

510   [30]   El-Kemary M, Rettig W. Multiple emission in coumarins with heterocyclic
511   substituents. Phys Chem Chem Phys 2003;5:5221–8.

512   [31]   Yamaguchi E, Wang C, Fukazawa A, Taki M, Sato Y, Sasaki T, Ueda M, Sasaki N,
513   Higashiyama T, Yamaguchi S. Environment-sensitive fluorescent probe: a
514   benzophosphole oxide with an electron-donating substituent. Angew Chem Int Ed
515   Engl 2015;54(15):4539–43.

516   [32]   Hagimori M, Mizuyama N, Shigemitsu Y, Wang BC, Tominaga Y. Development of
517   fluorescent 2-pyrone derivatives using ketene dithioacetals for organic EL devices.
518   Heterocycles 2009;78(3):555–70.

519   [33]   Sun Y, Sun Y, Zhao S, Cao D, Guan R, Liu Z, Yu X, Zhao X. Efficient solution- and
520   solid-state fluorescence for a series of 7-diethylaminocoumarin amide compounds.
521   Asian J Org Chem 2018;7:197–202.

522   [34]   Gaussian 09, Rev. A.2. Frisch MJ, Trucks GW, Schlegel HB, Scuseria GE, Robb MA,
523   Cheeseman JR, et al: Gaussian, Inc. Pittsburgh PA.

524   [35]   Becke, A.D. Becke's three parameter hybrid method using the LYP correlation
525   functional. J Chem Phys 1993;98:5648–52.

526   [36]   Yanai T, Tew DP, Handy NC. A new hybrid exchange–correlation functional using
527   the Coulomb-attenuating method (CAM-B3LYP). Chem Phys Lett 2004;393(1–3):
528   51–7.

529   [37]   Adamo C, Barone V. Toward reliable density functional methods without adjustable

530   parameters: The PBE0 model. J Chem Phys 1999;110:6158–69

531   [38]   Zhao Y, Truhlar DG. The M06 suite of density functionals for main group

532   thermochemistry, thermochemical kinetics, noncovalent interactions, excited states,

533   and transition elements: two new functionals and systematic testing of four M06-class

534   functionals and 12 other functionals. Theor Chem Acc 2008; 120: 215–41.

535   [39]   Yarkony DR. Conical intersections: Diabolical and often misunderstood. Acc Chem

536   Res 1998;31(8):511–8.

537   [40]   Werner HJ, Knowles PJ, Knizia G, Manby FR, Schütz M, et al. MOLPRO, version

538   2015.1, a package of ab initio programs, see http://www.molpro.net.

539   [41]   TURBOMOLE V7.1 2017, a development of University of Karlsruhe and

540   Forschungszentrum Karlsruhe GmbH, 1989-2007,TURBOMOLE GmbH, since 2007;

541   available fromhttp://www.turbomole.com.

542   [42]   Hagimori M, Matsui S, Mizuyama N, Yokota K, Nagaoka J, Tominaga Y. Novel

543   synthesis of 4H-quinolizine derivatives using sulfonyl ketene dithioacetals. Eur J Org

544   Chem 2009;2009(33):5847–53.

545   [43]   Hagimori M, Mizuyama N, Yokota K, Nishimura Y, Suzuta M, Tai CK, Wang BC,

546   Wang SL, Shih TL, Wu KD, Huang ZS, Tseng SC, Chen CY, Lu JW, Wei HH,

547   Kawashima K, Kawashima S, Tominaga Y. Synthesis of

548   6-(4-diethylamino)phenyl-2-oxo-2H-pyran-3-carbonitorile derivatives and their

549   fluorescence in solid state and in solutions. Dyes Pigm 2012;92(3):1069–74.

Table 1. UV and fluorescence data for **3–5** in solution (CHCl$_3$ and ethanol) and the solid state.

Compounds	Dissolved in CHCl$_3$			Dissolved in ethanol			Solid	
	λ_{max} (nm)[a]	Em$_{max}$ (nm)[b]	Φ[c]	λ_{max} (nm)[a]	Em$_{max}$ (nm)[b]	Φ[c]	Em$_{max}$ (nm)[b]	Φ[c]
3[d]	410	487	0.90	408	511	0.11	589	0.17
4	386	461	>0.99	384	491	0.61	524	0.03
5	384	461	0.12	384	491	0.05	533	0.18

Table 2. UV and fluorescence data for 2-substituted pyridine compounds **7–9** and **11** in solution ($CHCl_3$ and ethanol) and in the solid state.

Compounds	Dissolved in $CHCl_3$			Dissolved in ethanol			Solid	
	λ_{max} (nm)[a]	EM_{max} (nm)[b]	Φ[c]	λ_{max} (nm)[a]	EM_{max} (nm)[b]	Φ[c]	EM_{max} (nm)[b]	Φ[c]
7	386	455	0.95	386	487	0.62	475	0.15
8	388	459	0.83	386	491	0.59	436	0.12
9	348	410	0.64	346	426	0.23	441	0.39
11	386	435	0.87	382	465	0.88	491	0.19

[a]Concentration: 10^{-5}M. [b]Each emission was measured using excitation wavelengths. [c]This quantum yields were determined by using Absolute PL Quantum Yield Measurement System (C9920-01) of Hamamastu Photonics..

Table 3. UV-absorption and fluorescence properties of **4–9** and **11** in various solvents.

Solvent	λ_{max} (nm) (log e)					
	4	5	7	8	9	11
benzene	384 (4.68)	384 (4.64)	384 (4.46)	386 (4.68)	350 (4.52)	384 (4.59)
chloroform	386 (4.69)	386 (4.64)	386 (4.48)	388 (4.69)	348 (4.60)	386 (4.59)
acetone	380 (4.71)	384 (4.66)	382 (4.50)	386 (4.71)	346 (4.57)	380 (4.62)
ethanol	384 (4.67)	384 (4.66)	386(4.47)	386 (4.75)	346 (4.52)	382 (4.58)
acetonitrile	382 (4.68)	384 (4.65)	384 (4.48)	382 (4.69)	348 (4.54)	382 (4.59)
DMSO	392 (4.68)	392 (4.66)	392 (4.51)	392 (4.70)	352 (4.52)	388 (4.62)

Solvent	EM_{max} (nm) (Φ)					
	4	5	7	8	9	11
benzene	453 (0.92)	453 (0.07)	445 (0.87)	449 (0.78)	400 (0.28)	425 (>0.99)
chloroform	461 (>0.99)	461 (0.12)	455 (0.95)	459 (0.83)	410 (0.64)	435 (0.87)
acetone	489 (0.80)	489 (0.06)	485 (0.92)	485 (0.74)	410 (0.26)	447 (>0.99)
ethanol	491 (0.61)	491 (0.05)	487 (0.62)	491 (0.59)	426 (0.23)	465 (0.88)
acetonitrile	495 (0.71)	495 (0.06)	491 (0.84)	489 (0.69)	410 (0.33)	459 (>0.99)
DMSO	501 (0.64)	503 (0.05)	497 (0.72)	497 (0.63)	416 (0.76)	465 (0.94)

Table 4 Computed absoption λ_{max} (nm) and Oschillator strength f using several XC-functionals

Compounds	B3LYP		B3LYP in CHCl$_3$		CAM-B3LYP		PBEPBE		M06		M06-2X	
	λ_{max}	f	λ_{max}	f	λ_{max}	f	λ_{max}	f	λ_{max}	f	λ_{max}	f
4	377	0.77	409	0.93	330	0.97	440	0.55	366	0.82	331	0.98
5	374	0.54	415	0.57	331	0.65	447	0.32	362	0.59	331	0.67
7	370	0.73	396	0.87	323	0.97	444	0.40	360	0.78	325	0.97
8	380	0.57	403	0.85	335	0.67	437	0.43	370	0.62	337	0.69
9	363	0.44	379	0.81	319	0.65	414	0.34	352	0.56	320	0.67
11	382	0.63	404	0.88	336	0.71	441	0.39	371	0.66	337	0.73

Table 5 Computed absoption λ_{max} (nm) and Oschillator strength f using the two basis sets

Compounds	6-31+G**		6-311++G**	
	λ_{max}	f	λ_{max}	f
4	377	0.77	378	0.77
5	374	0.54	375	0.54
7	370	0.73	372	0.73
8	380	0.57	381	0.56
9	363	0.44	364	0.44
11	382	0.63	383	0.62

Table 6 Computed fluorescence λ_{max} (nm) and Oschillator strength f using several XC-functionals

Compounds	B3LYP		CAM-B3LYP		PBEPBE		M06		M06-2X	
	λ_{max}	f	λ_{max}	f	λ_{max}	f	λ_{max}	f	λ_{max}	f
4	351	0.03	337	0.00	415	0.02	349	0.03	312	0.03
5	363	0.24	349	0.26	460	0.02	435	0.02	352	0.18
7	386	0.95	344	1.11	446	0.69	377	0.98	345	1.12
8	392	0.82	347	1.00	457	0.47	383	0.86	348	1.01
9	372	0.79	334	1.03	421	0.57	365	0.9	335	1.03
11	402	0.77	347	1.00	482	0.51	388	0.83	348	0.99
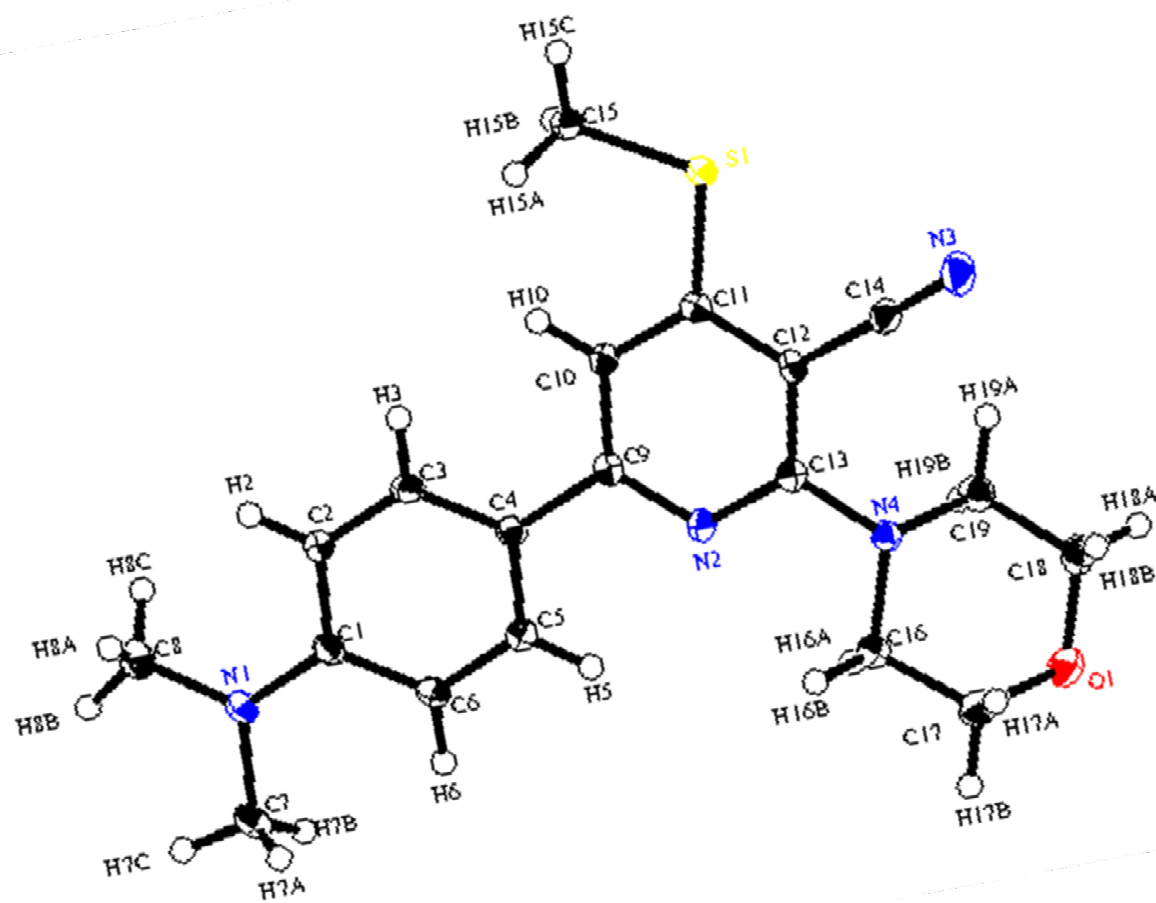
Fig. 1. ORTEP drawing of **8**.
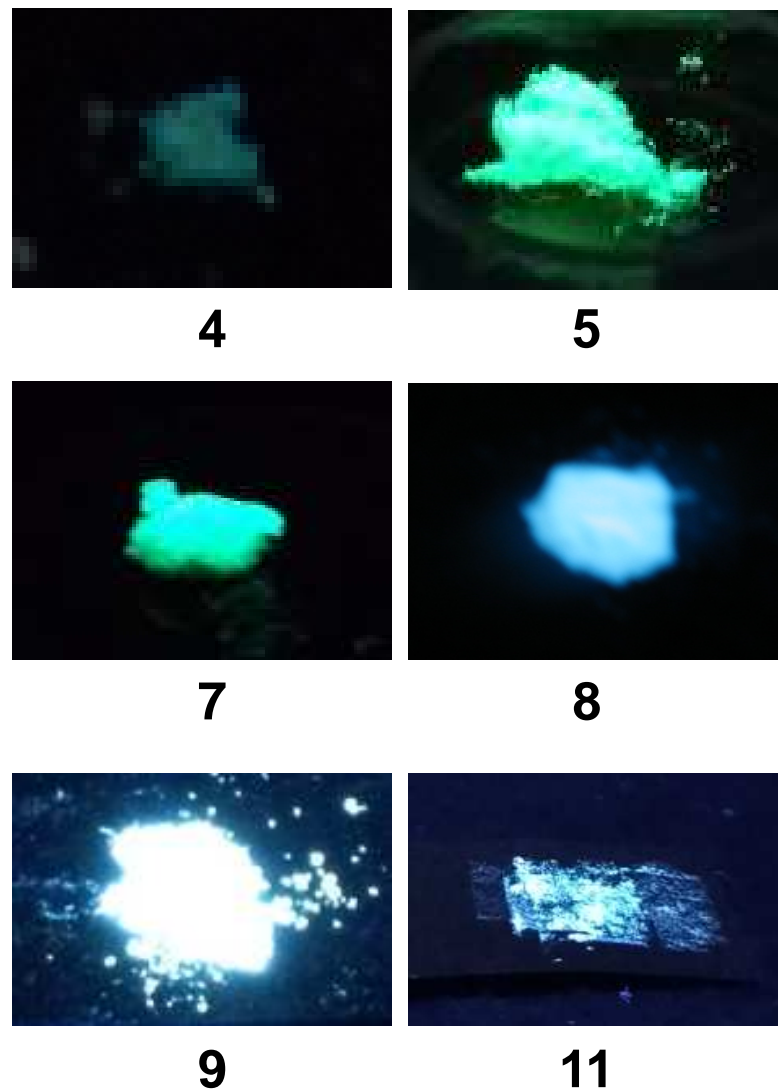
Fig. 2. Solid stare fluorescence photographs of **4,5, 7–9** and **11** irradiated with black light (365 nm).
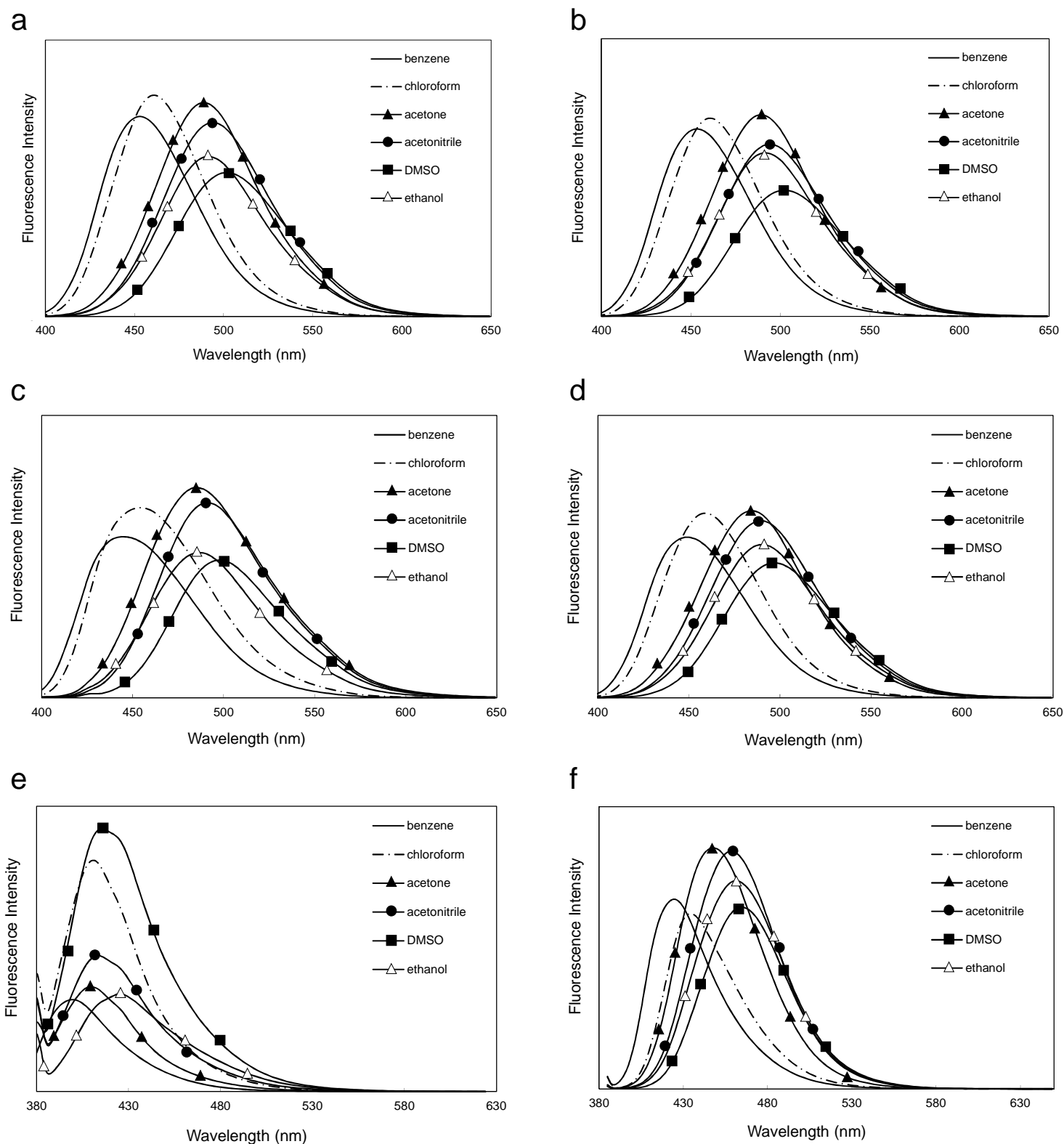
Fig. 3. Fluorescence spectra in benzene, chloroform, acetone, acetonitrile, DMSO, ethanol (1 x 10^{-5} M): (a) **4**, (b) **5**, (c) **7**, (d) **8**, (e) **9**, (f) **11**.
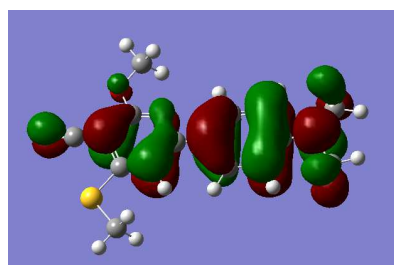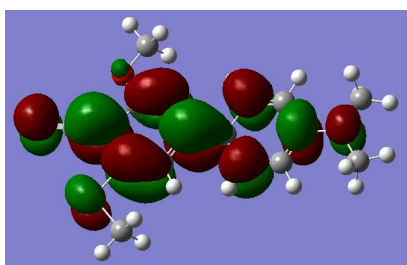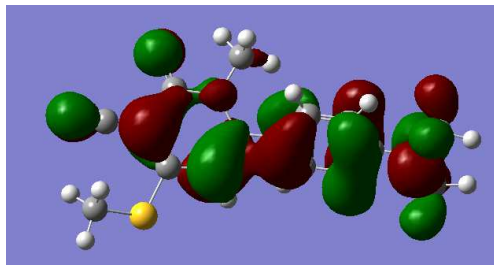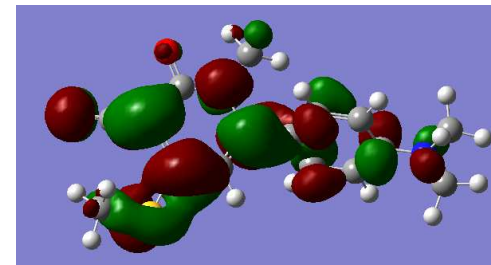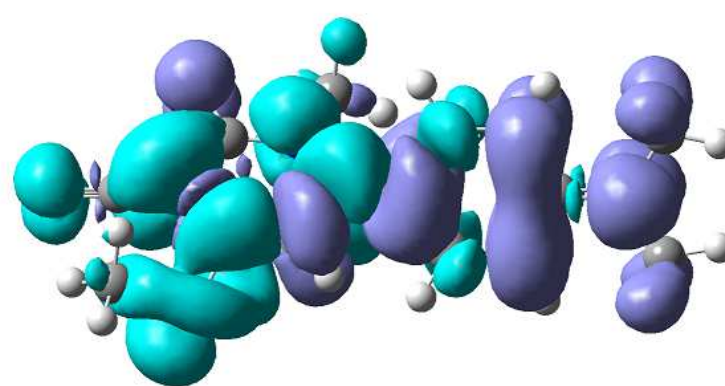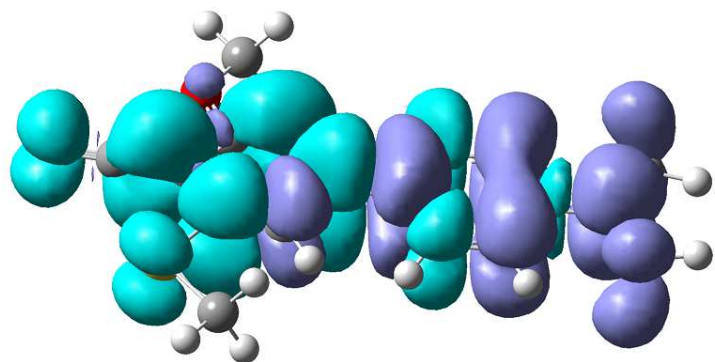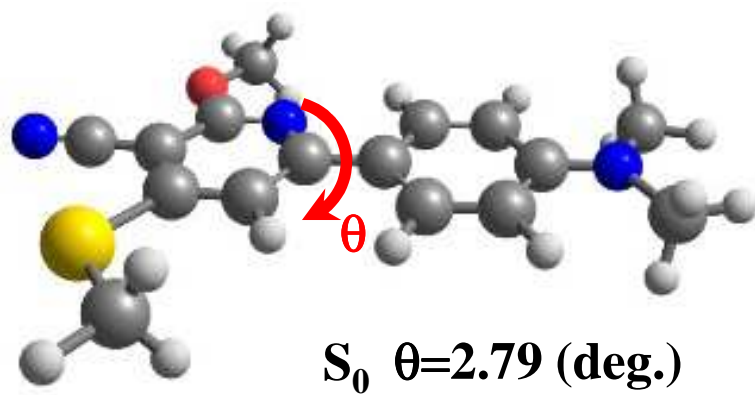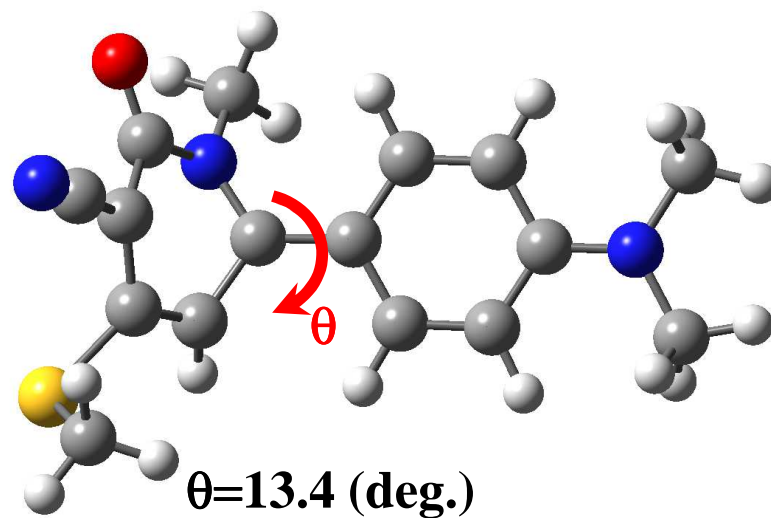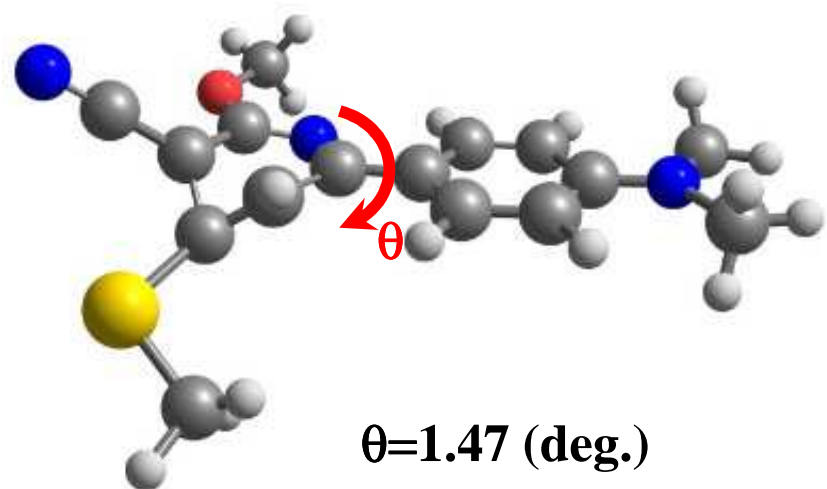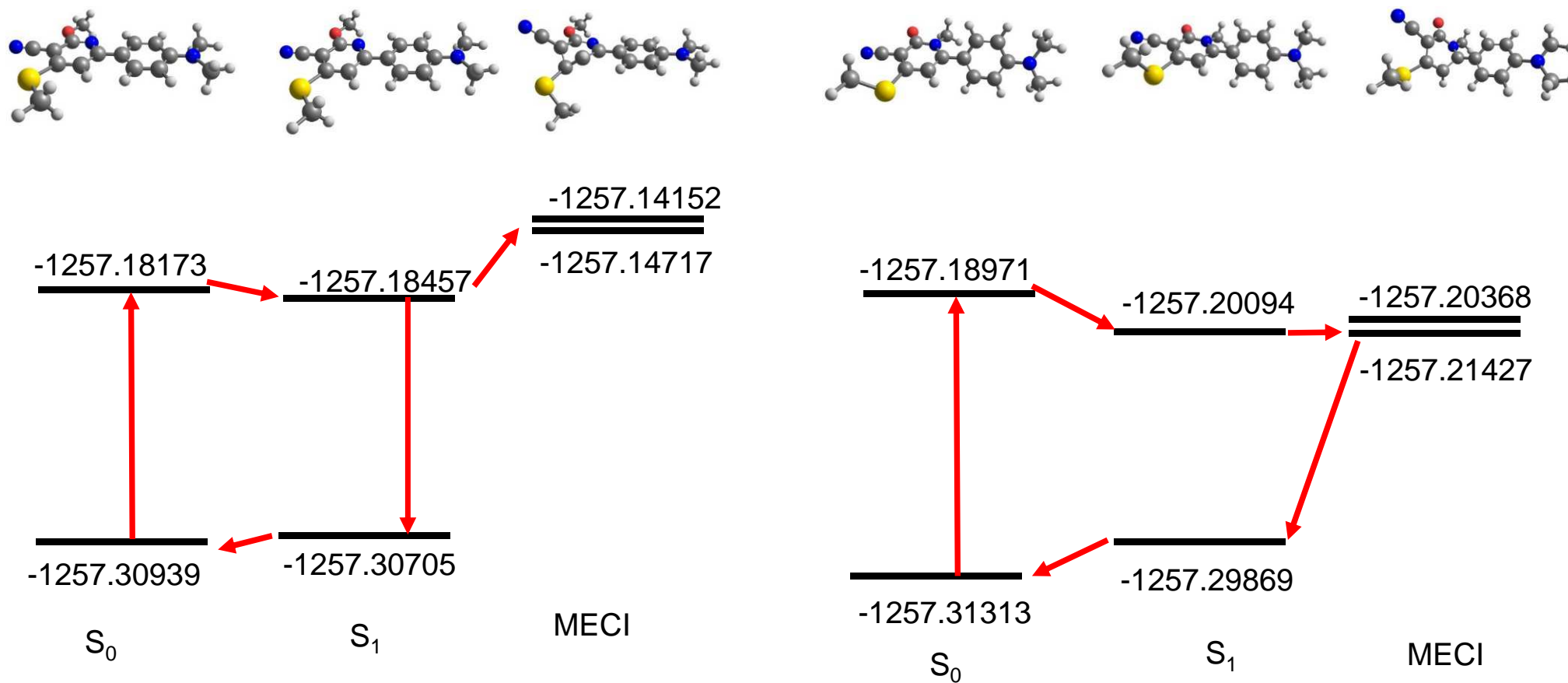
Fig. 4 HOMO, LUMO and S_0/S_1-electron density difference of **4** (left) and **5** (right)
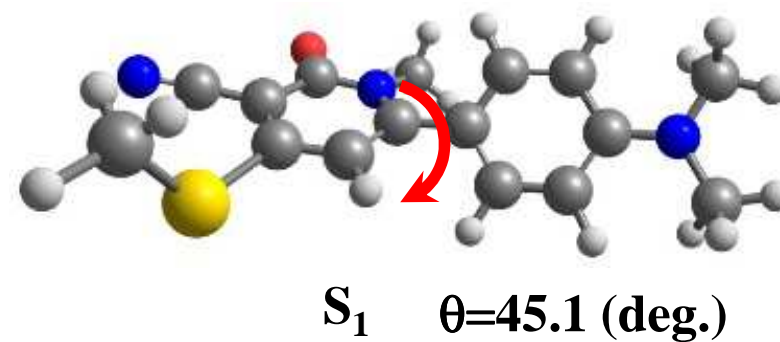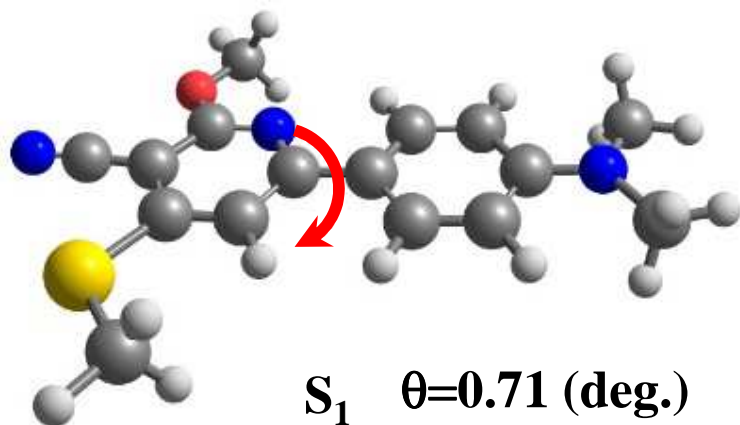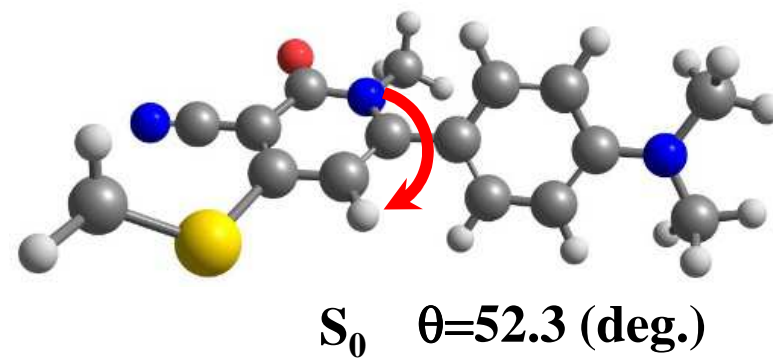
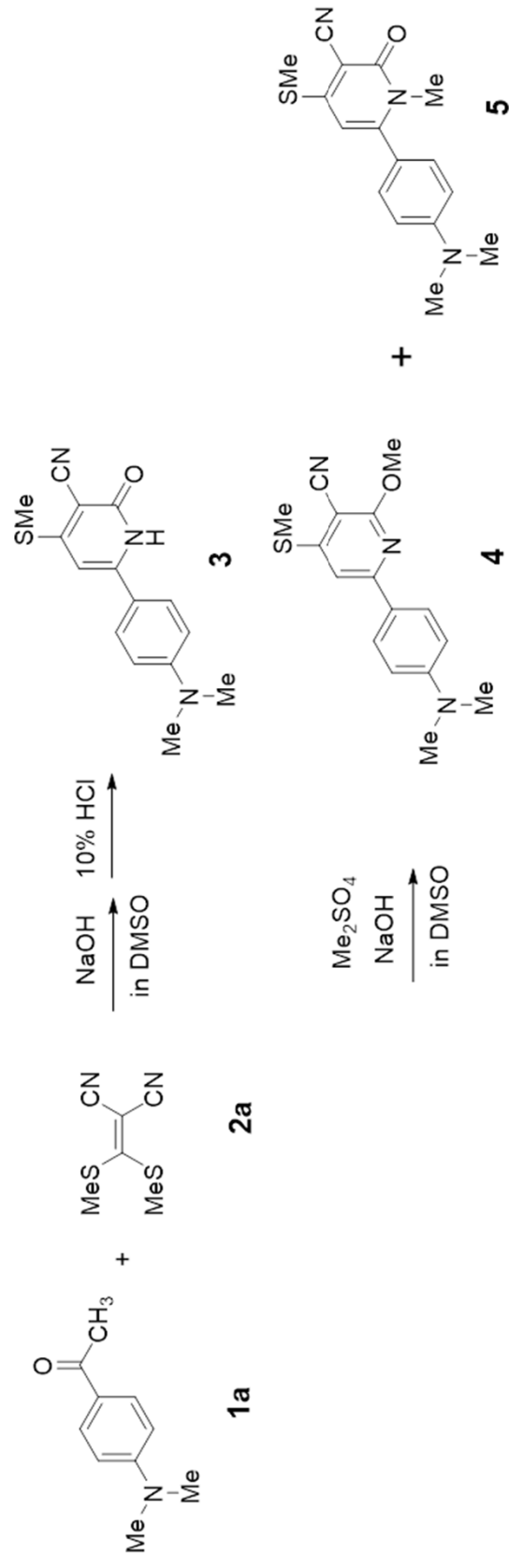**Fig. 5** The S_0, S_1 optimized geometry of **4** (left) and **5** (right)
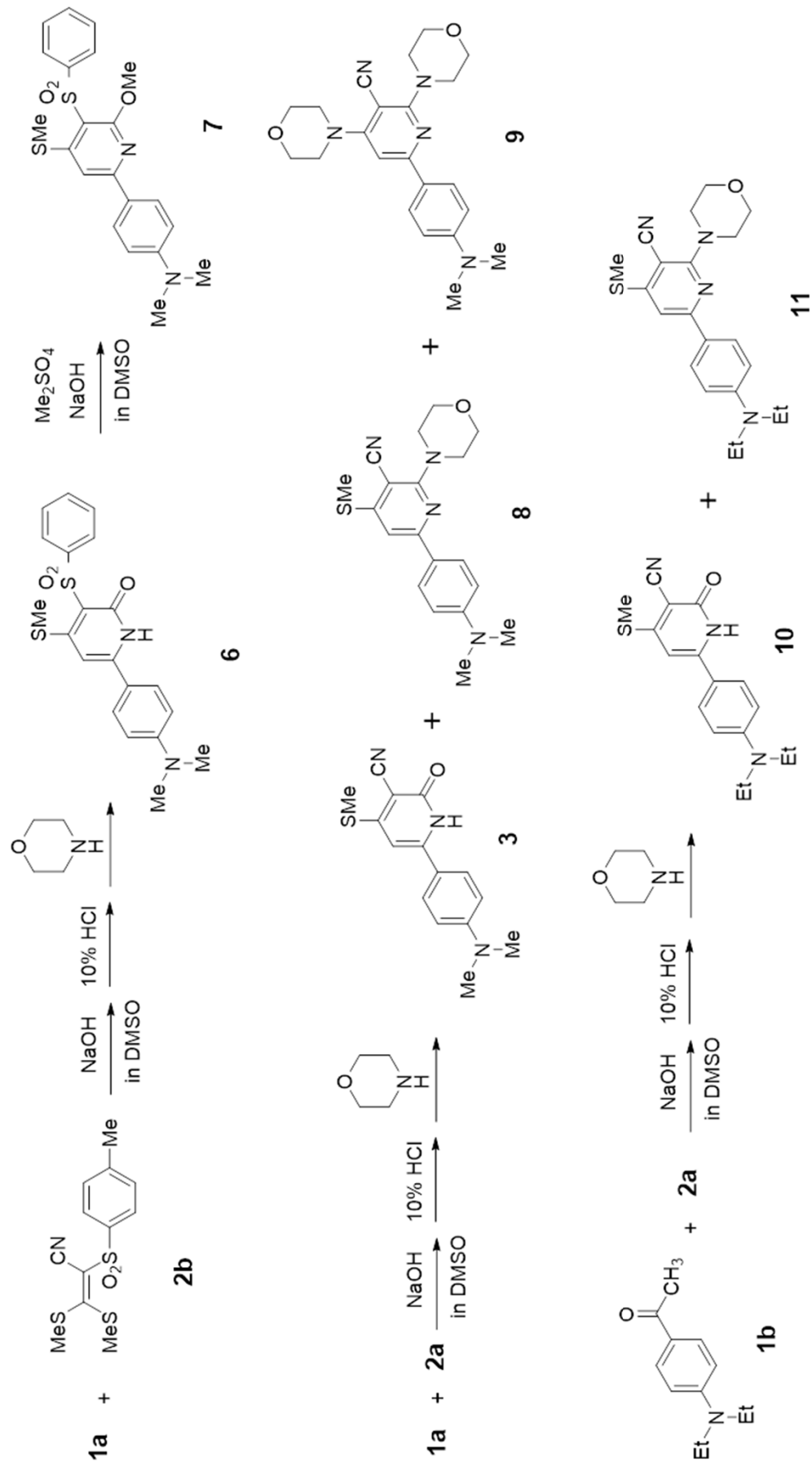
θ=1.47 (deg.)   θ=13.4 (deg.)

Fig. 6   MECI geometries of **4** (left) and **5** (right)

Fig. 7 The energy diagram of **4** (left) and **5** (right) (The energies in atomic unit.)

Scheme 1. Synthesis of methoxypyridine **4** and *N*-methylpyridone **5**.

Scheme 2. Synthesis of 2-substituted pyridine compounds **7–9** and **11**.

Highlights

► Joint experimental and computational studies of new 2-pyridone tautomeric compounds were performed.

► Strong fluorescence in solution is attributed to the enol form of the 2-pyridone.

► Methoxypyridine and morpholinopyridines exhibited solid-state fluorescence and a high fluorescence quantum yield in solution.

► Fluorescence solvatochromic effects depend on the chemical structure and arrangement of the substituents were observed.